

Solid-state Synthesis of High-Capacity $\text{LiNi}_{0.8}\text{Co}_{0.1}\text{Mn}_{0.1}\text{O}_2$ Cathode by Transition Metal Oxides

Hong-ren MAO¹, Ying-jie ZHANG^{2,*}, Peng DONG^{2,*}, Zhe-zhong SHI¹, Hui-xin LIANG²,
Jia-ming LIU²

¹ The Engineering Laboratory of Advanced Battery and Materials of Yunnan province, School of Material Science and Engineering, Kunming University of Science and Technology, Kunming 650093, China

² The Engineering Laboratory of Advanced Battery and Materials of Yunnan province, School of Metallurgical and Energy Engineering, Kunming University of Science and Technology, Kunming 650093, China

*E-mail: zyjkmust@126.com

Received: 30 August 2016 / Accepted: 21 September 2016 / Published: 10 November 2016

$\text{LiNi}_{0.8}\text{Co}_{0.1}\text{Mn}_{0.1}\text{O}_2$ cathode materials were synthesized using transition metal oxides in different synthesis conditions by solid-state reaction. Physical and electrochemical characterizations were made on the as-prepared $\text{LiNi}_{0.8}\text{Co}_{0.1}\text{Mn}_{0.1}\text{O}_2$ by X-ray diffraction, scanning electron microscope and charge-discharge test. All the examined samples have a good layered structure with $R\bar{3}m$ space group. $\text{LiNi}_{0.8}\text{Co}_{0.1}\text{Mn}_{0.1}\text{O}_2$ samples prepared with different lithium sources in different synthesis conditions exhibit different charge-discharge performances. The sample synthesized via the process of heating lithium nitrate and transition metal oxides at 400 °C for 8 h, followed by sintering at 800 °C for 24 h under O_2 atmosphere, exhibits a highest capacity of 210.5 mAh g^{-1} and capacity retention of 95.4% in 20 cycles at 0.2 C.

Keywords: Solid-state synthesis; transition metal oxides; synthesis conditions; lithium source

1. INTRODUCTION

For the demand for quality enhancement of people's life, it is necessary to search for renewable energies to replace the traditional ones according to the standards of energy-saving and environmental protection. In the pursuit of new energies, energy storage is a key issue. Lithium-ion battery is the best choice for this purpose for their advantages and can meet a variety of needs[1]. As a cathode, mixed oxide $\text{LiNi}_{1-x-y}\text{Co}_x\text{Mn}_y\text{O}_2$ is very promising. This mixed oxide inherits the merits of metal oxides,

LiCoO₂, LiNiO₂ and LiMnO₂, and has a lower cost, less toxicity, higher practical capacity, better cycle performance and improved structural stability[2-6]. Liu[7] reports the LiNi_{1-x-y}Co_xMn_yO₂ (0<x<0.5,0<y<0.5) structure for the first time. In order to get high-quality LiNi_{1-x-y}Co_xMn_yO₂, finding out suitable Ni, Co, and Mn sources and a homogeneous mixing of starting materials is very important. The most frequently used Ni, Co, and Mn sources are sulfates, chlorides, etc[2,3,4,8], and commonly used lithium sources are LiOH·H₂O, LiNO₃, Li₂CO₃, Li(CH₃COO)·2H₂O, etc[5].

LiNi_{0.8}Co_{0.1}Mn_{0.1}O₂ powders could be prepared by various synthesis methods, such as co-precipitation[9,10], sol-gel[10], solution combustion, PVA precursor and spray pyrolysis[8]. Among these methods, co-precipitation and sol-gel are the most common ways, and they are a typical method of liquid phase route. A liquid method is advantageous to an even transition metals distribution and preferred morphology and particle size in material particles if the experimental conditions are correctly and strictly controlled. HU Guo-rong[11] prepared LiNi_{0.8}Co_{0.1}Mn_{0.1}O₂ by co-precipitation that delivers an initial discharge capacity of 195.4 mAh g⁻¹ in 3.0-4.3 V at 0.2 C. LI[12] prepared LiNi_{0.8}Co_{0.1}Mn_{0.1}O₂ by co-precipitation demonstrating an initial discharge capacity of 192.4 mAh g⁻¹ in 3.0-4.3 V at 0.2 C. Nevertheless, a liquid route is disadvantageous due to the necessary but troublesome aging, stirring, unceasing filtering and washing, and drying. The process is both time and energy consuming. What is more, a lithiation is needed to produce the aimed product. For mass production of cathode materials a solid state method is suitable. The method is simple in operation and has a lower demand for apparatuses. Meanwhile, the transition metal and lithium sources can be mixed according to a precise stoichiometry at the outset. This may lead to a high capacity. However, the solid state method has the shortcoming that in mixing starting materials, lithium sources and transition metals can not be uniformly mixed. It may affect unfavorably the mass transfer in the succeeding solid state reaction at an elevated temperature.

A rigorous grinding of raw materials could be done to tackle problems in mixing. In the meantime, a strictly-controlled calcination could be done to treat the mixed raw materials to get a loose and porous product under oxygen in muffle furnace. In the paper, the optimum conditions for LiNi_{0.8}Co_{0.1}Mn_{0.1}O₂ material preparation will be attained by detailed studies on the pre-sintering temperature, calcination temperature and different lithium sources. The effect of calcination temperature on the electrochemical properties of LiNi_{0.8}Co_{0.1}Mn_{0.1}O₂ material will be specifically discussed.

2. EXPERIMENTAL

LiNi_{0.8}Co_{0.1}Mn_{0.1}O₂ was prepared by solid-state reaction route with lithium hydroxide or lithium nitrate, Ni₂O₃, Co₃O₄ and MnO₂. Three different processes were used with each lithium source. In process A, stoichiometric lithium hydroxide and transition metal oxides were ground with mortar and pestle for 3 h. The ground mixture was calcined at 800 °C and 900 °C, respectively, in an O₂ atmosphere for 24 h to obtain LiNi_{0.8}Co_{0.1}Mn_{0.1}O₂ samples A₁ and A₂. In process B based on process A, the ground mixture was sintered at 300-700 °C in air for 8 h, and then the sintered product was ground again and calcined at 800 °C in O₂ atmosphere for 24 h to obtain LiNi_{0.8}Co_{0.1}Mn_{0.1}O₂ samples

B₁, B₂, B₃, B₄ and B₅ (subscripts 1, 2, 3, 4 and 5 refer to 300 °C, 400 °C, 500 °C, 600 °C and 700 °C, respectively). Process C differed from process B in calcination temperature of 900 °C and obtained samples C₁, C₂, C₃, C₄ and C₅. Following the above processes, lithium nitrate was used to replace lithium hydroxide to obtain LiNi_{0.8}Co_{0.1}Mn_{0.1}O₂ samples A₁' , A₂' , B₁' , B₂' , B₃' , B₄' , B₅' , C₁' , C₂' , C₃' , C₄' and C₅'.

The synthesized LiNi_{0.8}Co_{0.1}Mn_{0.1}O₂ was examined by X-ray diffraction (XRD, MiniFlex-600, Rigaku) using Cu K α radiation. Diffraction data were collected from 10° to 80° with a step of 0.02°. The XRD patterns were indexed and intensity ratio $I_{(003)}/I_{(104)}$ are calculated using Rietveld analyses, although it was not accurate in the present case but to a very approximation the intensities of the XRD fingerprint peaks can predict cation mixing[13-15]. The morphology of cathode materials was observed with scanning electron microscope (SEM, Teacan Vega3).

The charge-discharge capacities of LiNi_{0.8}Co_{0.1}Mn_{0.1}O₂ cathode were measured by using 2016 button cells with a lithium metal anode and Celgard 2400 microporous membrane. The cathode was fabricated by blending LiNi_{0.8}Co_{0.1}Mn_{0.1}O₂, carbon black and PVDF (80:10:10 by weight) in N-methyl-2-pyrrolidone. The resultant slurry was symmetrically spread on an aluminum foil with a coating machine and dried in vacuum at 120 °C. The electrolyte was 1mol/L LiPF₆ in a mixed solvent of dimethyl carbonate (DMC), ethylene carbonate (EC), ethylmethyl carbonate (EMC) at a volume ratio of 1:1:1. The coin cell was assembled in a dry Ar atmosphere glove box. The charge-discharge test was carried out using LAND-CT2001A test system in the potential rang of 3.0-4.35 V at 0.2 C at a temperature of 25 °C.

3. RESULTS AND DISCUSSION

X-ray diffraction patterns of the LiNi_{0.8}Co_{0.1}Mn_{0.1}O₂ powder prepared in different synthesis conditions are shown in Fig. 1. It can be observed that the major characteristic peaks for all the samples in the diffraction pattern are spiculate, indicating a good crystallinity, and they are located at the identical degrees in the reported literature on layered materials[16]. The layered structure belongs to space group $R\bar{3}m$ and is isostructural with hexagonal α -NaFeO₂. Meanwhile, all the samples show not impurity phases. Fig. 1 indicates that the split of the (006/102) and (108/110) doublets becomes more distinct with increased pre-sintering and calcining temperatures. $I_{(003)}/I_{(104)}$ values for cathodes are calculated and given in Table 1. Because the ionic radius of Ni²⁺(0.70Å) is very close to that of Li⁺(0.76Å), an occupation of Ni²⁺ in the Li⁺ layer is highly possible [17], To a certain extent, $I_{(003)}/I_{(104)}$ value is a parameter determining the cation distribution in layered oxide lattice. Usually, a higher value than 1.2 means a low level cation mixing, which will be advantageous to the lithium-ion transfer in electrochemical processes[9], and vice versa. In general, cation mixing is directly affected by a synthesis process[18]. From Table 1, it can be observed that, in the same pretreatment process, materials made with lithium hydroxide and calcined at 900 °C and those made with lithium nitrate and calcined at 800 °C exhibit an irregular $I_{(003)}/I_{(104)}$ value change, but there is a decrease trend in general with an increased pre-sintering and calcining temperatures. Therefore, different lithium sources and calcining temperatures lead to lattice differences for LiNi_{0.8}Co_{0.1}Mn_{0.1}O₂ samples. Among all the

samples, A₁, A₂, A₁' , A₂' , B₁, B₂, B₃, B₁' , B₂' , B₃' , C₁, C₂ and C₁' exhibit a $I_{(003)}/I_{(104)}$ value higher than 1.2, endowing a better layeredness and lower cation mixing. B₄, B₅, C₄, C₅, B₅' , C₃' , C₄' and C₅' with an even lower $I_{(003)}/I_{(104)}$ value are shown when compared with other samples. A possible reason is that LiOH remains reacted with nitrogen oxide gas during the high temperature synthetic process[19].

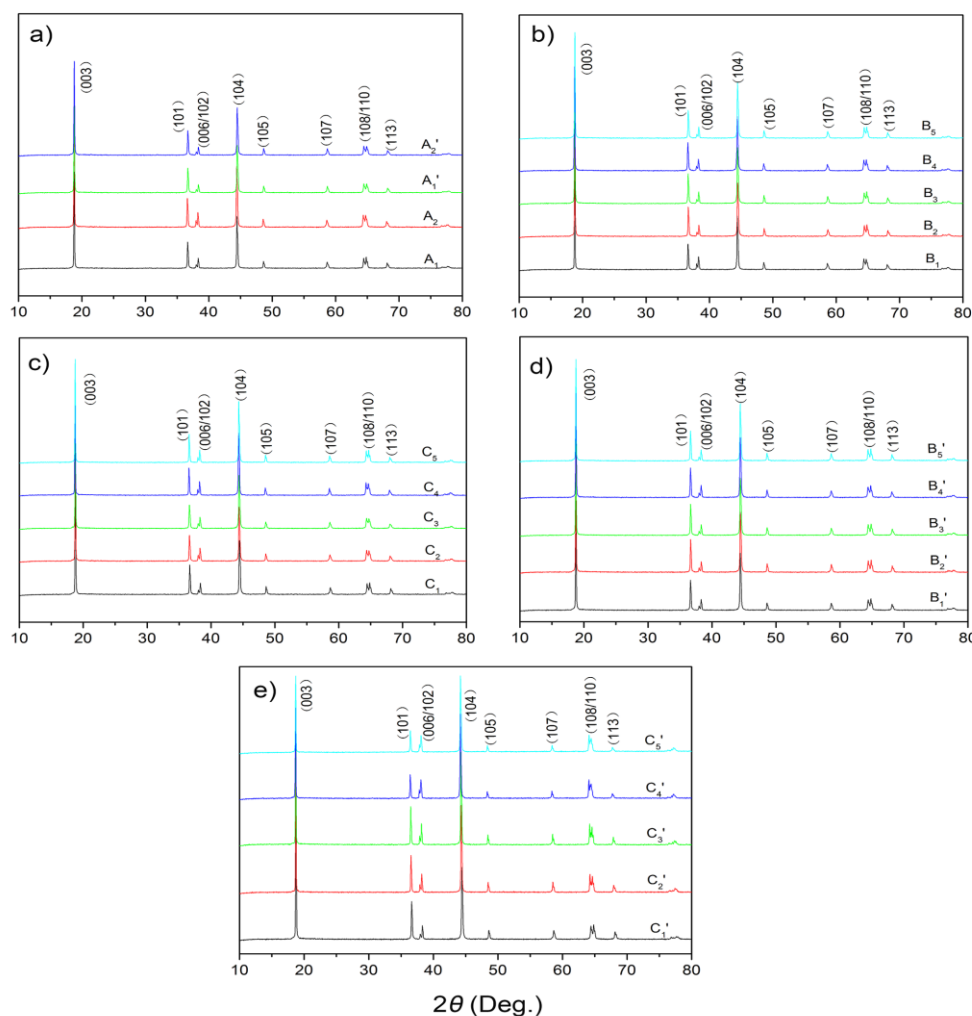


Figure 1. XRD patterns of $\text{LiNi}_{0.8}\text{Co}_{0.1}\text{Mn}_{0.1}\text{O}_2$ obtained in different synthesis conditions.

Fig. 2 shows the SEM images of $\text{LiNi}_{0.8}\text{Co}_{0.1}\text{Mn}_{0.1}\text{O}_2$ samples prepared in different synthesis conditions by solid-state reaction. As can be seen from Fig. 2 a, b, c and d, adoption of lithium hydroxide as a lithium source leads to $\text{LiNi}_{0.8}\text{Co}_{0.1}\text{Mn}_{0.1}\text{O}_2$ samples with a similar spherical morphology and average particle size about 3-5 μm . However, the morphology changes with synthesis conditions. A₂ and C₃ exhibit bigger particle sizes than A₁ and B₃. A₂ and C₃ show agglomeration when compared with A₁ and B₃. A₂ has biggest-sized particles and B₃ has smallest-sized particles. B₃ has a narrow particle size range, which may benefit its electrochemical performance. A₂' and C₂' demonstrate a greater particle size than A₁' and B₂'. A₂' and C₂' have a wider size distribution compared with A₁' and B₂'. C₂' has biggest-sized particles and B₂' has smallest-sized particles. B₂' has an even

size distribution. Aggregation becomes severe with increased pre-sintering and calcining temperatures. A smaller particle size provides shorter Li^+ diffusion paths, which can improve capacity and reversibility of an electrode material with low electronic conductivity.

Table 1. $I_{(003)}/I_{(104)}$ values of the samples prepared in different synthesis conditions.

Sample	Pre-sintering temperature	Calcining temperature	$I_{(003)}/I_{(104)}$
A ₁	/	800	1.23
A ₂	/	900	1.39
A ₁ '	/	800	1.27
A ₂ '	/	900	1.24
B ₁	300	800	1.39
B ₂	400	800	1.37
B ₃	500	800	1.23
B ₄	600	800	1.19
B ₅	700	800	1.17
C ₁	300	900	1.37
C ₂	400	900	1.39
C ₃	500	900	1.19
C ₄	600	900	1.06
C ₅	700	900	1.08
B ₁ '	300	800	1.24
B ₂ '	400	800	1.30
B ₃ '	500	800	1.21
B ₄ '	600	800	1.12
B ₅ '	700	800	1.16
C ₁ '	300	900	1.24
C ₂ '	400	900	1.04
C ₃ '	500	900	1.16
C ₄ '	600	900	0.71
C ₅ '	700	900	0.67

Therefore, particle morphology and size control are necessary[6,12]. Small-sized particles with narrow size distribution are preferred for the layered cathode material. A charge-discharge test will be carried out in the following to find optimum synthesis conditions for high-quality $\text{LiNi}_{0.8}\text{Co}_{0.1}\text{Mn}_{0.1}\text{O}_2$ preparation.

The initial charge-discharge and cycling performance of $\text{LiNi}_{0.8}\text{Co}_{0.1}\text{Mn}_{0.1}\text{O}_2$ samples in 3.0-4.35 V at 0.2 C are shown in Fig. 3. It is noted that the average capacity and average discharge voltage decrease with increased calcining temperatures. For A_1 , A_2 , A_1' and A_2' , the initial capacities are 142.3, 134.8, 135.7 and 63.2 mAh g^{-1} , the average values are 123.8, 82.5, 93.3 and 35.6 mAh g^{-1} , and the capacity retentions are 80.1%, 40.7%, 55.2% and 37.9%, respectively, in 20 cycles. It is apparent that A_1 exhibits the highest capacity and best capacity retention and its capacity is 114 mAh g^{-1} after 20 cycles. However, the samples obtained with higher pre-treatment temperatures show inferior performances. A_2' shows a very low capacity and poor capacity retention, with a capacity only 24 mAh g^{-1} after 20 cycles. A_2 and A_1' have similar initial capacities, but A_1' has a higher average capacity and better capacity retention. The negative effect of high temperature pretreatment is obvious when it is increased to 800 °C. A possible reason is that a high temperature may lead to a more severe aggregation in material particles.

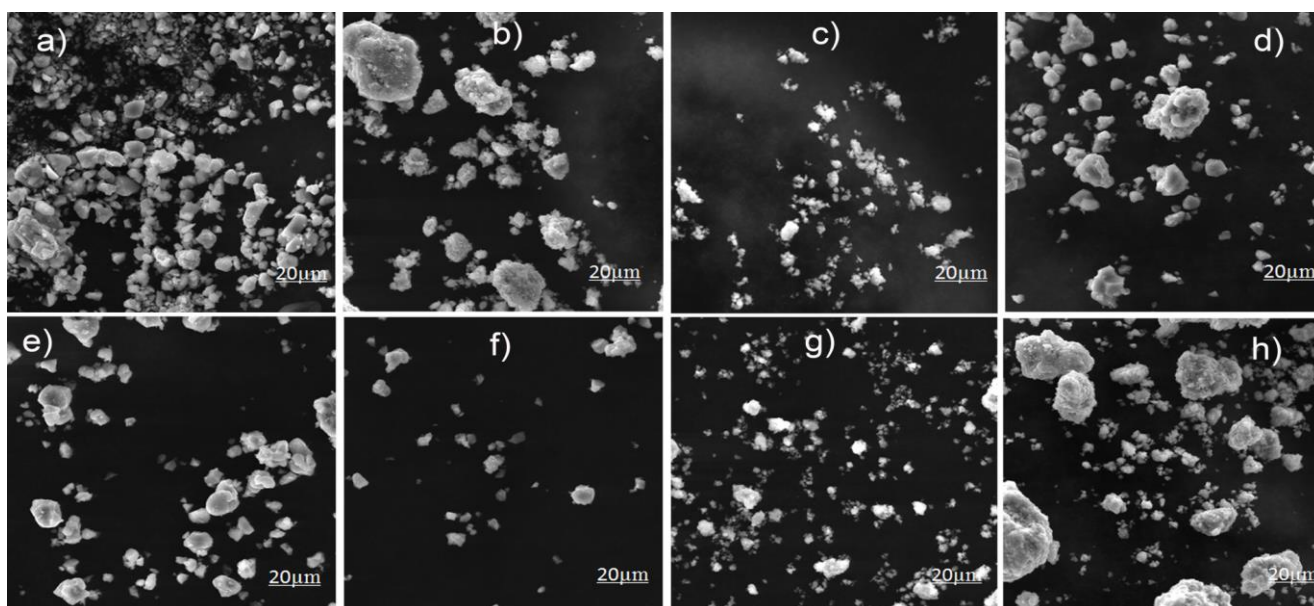


Figure 2. SEM images of $\text{LiNi}_{0.8}\text{Co}_{0.1}\text{Mn}_{0.1}\text{O}_2$: (a) A_1 ; (b) A_2 ; (c) B_3 ; (d) C_3 ; (e) A_1' ; (f) A_2' ; (g) B_2' ; (h) C_2' .

B_1 , B_2 , B_3 , B_4 and B_5 exhibit initial capacities of 167.9, 172.8, 195, 171.5 and 168.9 mAh g^{-1} , and highest capacities of 167.9, 173.4, 195.8, 171.6 and 171.5 mAh g^{-1} , average capacities of 138.4, 165.4, 181.1, 158.0 and 164.1 mAh g^{-1} and capacity retentions of 80.3%, 90.3%, 83.5%, 85.1% and 93.9%, after 20 cycles, respectively. B_1 , B_5 , B_2 and B_4 exhibit close initial capacities, B_2 , B_4 and B_5 have similar highest capacities, and B_2 and B_5 have nearly equal capacity retentions. Meanwhile, from the initial discharge capacities it can be observed that the capacities first increase and then decrease with increased pre-sintering temperatures. This may be ascribed to a lower cation mixing given rise to by a lower pretreatment temperature. A higher pretreatment temperature may lead to a higher cation mixing and also a more severe aggregation in particles. B_3 exhibits the highest capacities and a capacity of 162.9 mAh g^{-1} after 20 cycles, which is better than others in this group. When compared with the samples synthesized without any pretreatment, materials obtained with a pretreatment deliver

a higher capacity and better capacity retentions. Therefore, heating pretreatment may be beneficial to preparation of better ternary oxide materials.

C₁, C₂, C₃, C₄ and C₅ demonstrate first and highest discharge capacities of 153.5, 158.7, 163.1, 121.2 and 145.6 mAh g⁻¹, average capacities of 142.7, 149.9, 141.6, 94.1 and 133.4 mAh g⁻¹, and capacity retentions of 88.7%, 89.9%, 79.8%, 68.7% and 86.2%, after 20 cycles, respectively. C₄ exhibits the poorest performance possibly due to a high cation mixing and large particle size, as confirmed by X-ray diffraction and scanning electron microscopy. C₁, C₂ and C₅ have close capacity retentions, but C₂ exhibits a marked capacity fluctuation on cycling, which may be explained by the structural instability on lithiation and delithiation. C₄ exhibits a very inferior electrochemical performance due to the possible severe lithium loss in pre-sintering and calcining, which may induce an increased cation disorder and incomplete layered structure. C₃ has the highest initial capacity, but its capacity decreases fast on cycling. This may be imputable to the increased calcining temperature leading to a big particle size compared with B₃. In general, a lower capacity and inferior electrochemical performance is delivered by samples synthesized with process C in comparison with samples prepared with process B.

B₁' , B₂' , B₃' , B₄' and B₅' exhibit initial capacities of 169.7, 207.3, 178.2, 141.9 and 161.3 mAh g⁻¹, highest capacities of 173.5, 210.5, 179.1, 150.3 and 164.1 mAh g⁻¹, average capacities of 170.4, 205.1, 172.2, 143.1 and 157.9 mAh g⁻¹, and capacity retentions of 98.7%, 95.4%, 92.1%, 97.3% and 93.4% after 20 cycles, respectively. B₁' and B₃' have similar average capacities and highest capacities. B₁' and B₅' have similar initial capacities, but the former has a higher average capacity and highest capacity. B₄' displays better capacity retention, but its initial capacity is lower than the other four samples. All of the results are consistent with $I_{(003)}/I_{(104)}$ values. B₂' exhibits the highest initial and highest capacities and capacity retention. Those capacities are higher than what reported in literature[5,6]. B₁' , B₂' , B₃' , B₄' and B₅' exhibit improved capacities and retentions in comparison with the samples obtained using lithium hydroxide as a lithium source. The improved cycling performance indicates that a low temperature pre-treatment can improve the particle morphology, cation distribution and structural stability[20]. These improvements are beneficial to Li⁺ intercalation/de-intercalation[21], but a further increased temperature may lead to a larger particle size and cation mixing, as can be seen in Table 1.

C₁' , C₂' , C₃' , C₄' and C₅' exhibit initial capacities of 68.9, 121.1, 105, 40.3 and 41.6 mAh g⁻¹, highest capacities of 68.9, 121.1, 105, 40.3 and 41.6 mAh g⁻¹ and average capacities of 40.4, 92.2, 60.5, 21.3 and 16.4 mAh g⁻¹ after 20 cycles, respectively. The poor capacity retentions are consistent with characterization results in Table 1. C₁' , C₂' , C₃' , C₄' and C₅' have low $I_{(003)}/I_{(104)}$ values, which to a certain extent can be regarded as a high lattice disorder. Meanwhile, scanning electron microscopy shows larger particle sizes for this group than others. Their very inferior electrochemical performances are associated with the fact that an increased temperature causes high cation disorder, morphology deformity and severe aggregation.

In order to enrich the research, we also adopted lithium acetate and lithium carbonate as lithium sources for LiNi_{0.8}Co_{0.1}Mn_{0.1}O₂ synthesis. Though they have been reported as good choices for Li, in our research they failed to achieve high-performance cathode materials.

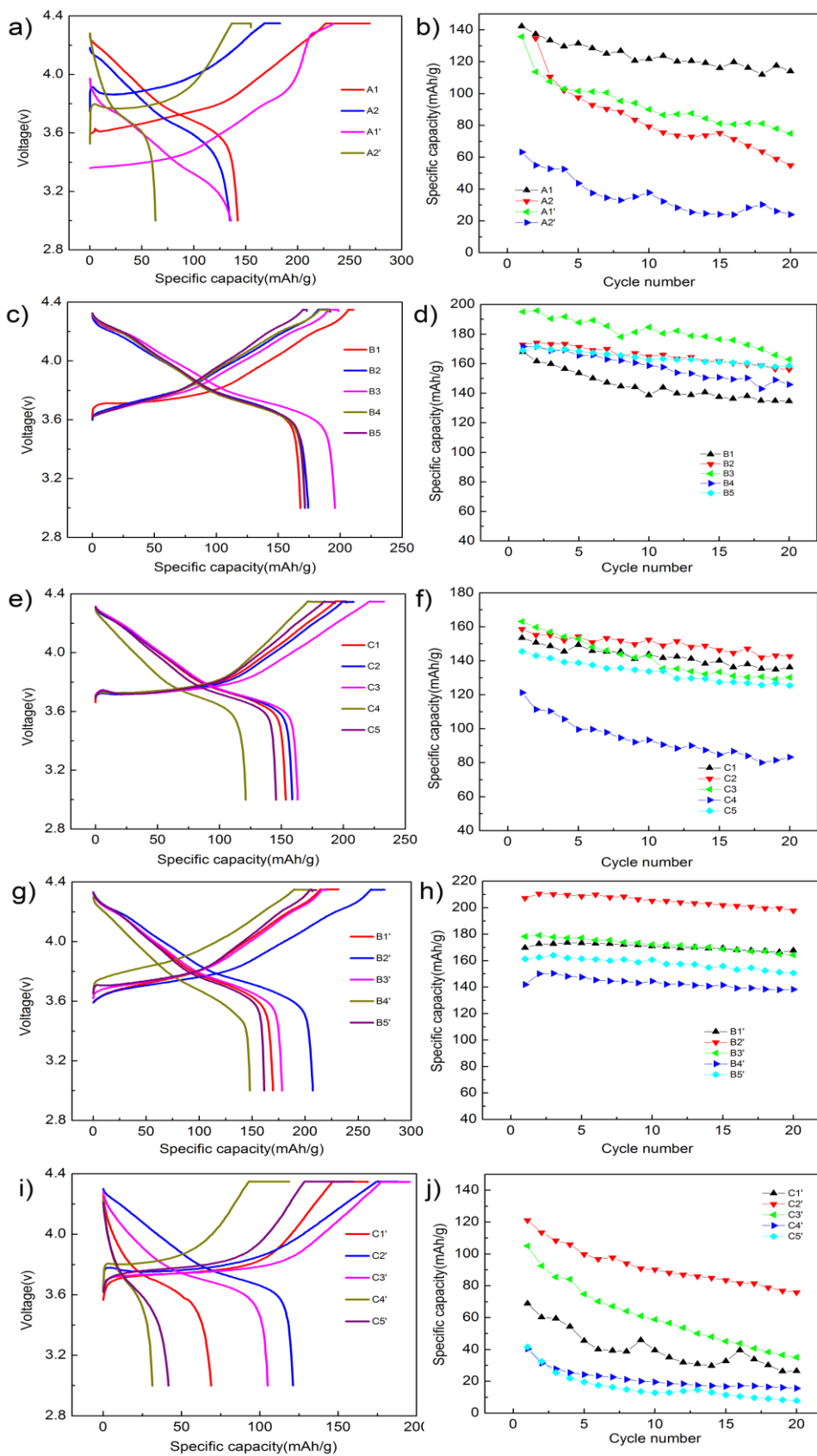


Figure 3. The initial charge-discharge curve and cycling performance for as-prepared $\text{LiNi}_{0.8}\text{Co}_{0.1}\text{Mn}_{0.1}\text{O}_2$ (a)-(j) in different conditions between 3.0 and 4.35 V at 0.2 C.

Tests show that the mixed layered oxides made from the two lithium sources exhibit higher cation mixing and very large particle sizes. However, our work has never eliminated their possibility of being used for synthesis of high-capacity $\text{LiNi}_{0.8}\text{Co}_{0.1}\text{Mn}_{0.1}\text{O}_2$. Among all the samples, B_1' exhibits the highest capacity retention of 98.7% after 20 cycles and comparatively high $I_{(003)}/I_{(104)}$ value, but its initial and highest capacities are lower than B_2' . B_2' delivers excellent electrochemical performance, in agreement with its comparatively high $I_{(003)}/I_{(104)}$ value and small particle size. C_5' exhibits a very inferior electrochemical performance and capacity retention compared with others. A possible reason is that lithium nitrate has a melting point of 255 °C and a boiling point of 600 °C. When the temperature reaches 255 °C, lithium nitrate will melt and tend to vaporize. This will be unfavorable to lithium maintenance and lead to a high cation disorder and inferior layeredness. More particular reasons need to be revealed by further tests and analyses.

The above shows that a low temperature pre-sintering of transition metal oxides and a lithium source, followed by a high temperature calcination under O_2 atmosphere, may synthesize $\text{LiNi}_{0.8}\text{Co}_{0.1}\text{Mn}_{0.1}\text{O}_2$ with increased discharge capacity and cycling stability compared with the samples obtained without any pretreatment adoption. The phenomenon is more apparent when lithium nitrate was used as a lithium source. Meanwhile, more experiments should be done to know the reasons why the use of lithium acetate and lithium carbonate only achieved materials with unusual and unexplainable electrochemical test results.

Among all the samples, B_3 and B_2' exhibit the best electrochemical performance. Improvement on cathode's performance can be made by further optimization of synthesis conditions for the innate reasons in solid-state, such as inhomogeneous mixing of raw materials and irregular morphology of material particles. For example, ball-milling and morphology control can be utilized. Meanwhile, other strategies, including surface modification and doping, can be adopted in the subsequent work to prepare high-quality $\text{LiNi}_{0.8}\text{Co}_{0.1}\text{Mn}_{0.1}\text{O}_2$.

4. CONCLUSIONS

1) $\text{LiNi}_{0.8}\text{Co}_{0.1}\text{Mn}_{0.1}\text{O}_2$ cathode materials were synthesized using transition metal oxides in different synthesis conditions by solid-state reaction. All the samples exhibited layered structure with $R\bar{3}m$ space group as in $\alpha\text{-NaFeO}_2$ and an average particle size of 3-5 μm . A part of samples delivered very good electrochemical performances.

2) $\text{LiNi}_{0.8}\text{Co}_{0.1}\text{Mn}_{0.1}\text{O}_2$ obtained by pre-sintering transition metal oxides and lithium hydroxide at 500 °C and then calcination at 800 °C showed a highest capacity of 195.8 mAh g^{-1} and average of 181.1 mAh g^{-1} in 20 cycles at 0.2 C. The mixture of transition metal oxides and lithium nitrate pre-sintered at 400 °C and then calcined at 800°C gave rise to a sample delivering a highest capacity of 210.5 mAh g^{-1} and average of 205.1 mAh g^{-1} in 20 cycles at 0.2 C.

3) Adoption of lithium acetate and lithium carbonate as a lithium sources for synthesizing high-quality $\text{LiNi}_{0.8}\text{Co}_{0.1}\text{Mn}_{0.1}\text{O}_2$ were unsuccessful. Transition metal oxides were suitable for high-capacity $\text{LiNi}_{0.8}\text{Co}_{0.1}\text{Mn}_{0.1}\text{O}_2$ preparation. The work laid a foundation for further improvement at cathode's performance by synthesis condition optimization and other strategies.

ACKNOWLEDGEMENTS

This paper was finished by Project supported by the National Natural Science Foundation of China (Grant No. 51364021) and Project supported by the Natural Science Foundation of Yunnan Province (2014FA025).

References

1. B. L. Ellis, K. T. Lee and L. F. Nazar, *Chem. Mater.*, 22 (2010) 691-714.
2. S. Y. Yang, X. Y. Wang, X. K. Yang, Z. L. Liu, Y. S. Bai, Y. P. Wang and H. B. Shu, *J. Solid State. Electrochem.*, 16 (2012) 2823-2836.
3. L. J. Li, X. H. Li, Z. X. Wang, H. J. Guo, P. Yue, W. Chen and L. Wu, *J. Alloys compd.*, 507 (2010) 172-177.
4. L. J. Li, X. H. Li, Z. X. Wang, L. Wu, J. H. Zheng and J. H. Li, *Trans. Nonferrous Met. Soc China.*, 20 (2010) s279 -s282.
5. Z. W. Xiao, Y. J. Zhang and Y. F. Wang, *Trans. Nonferrous Met. Soc China.*, 25 (2015) 1568-1574.
6. J. J. Saavedra-Arias, N. K. Karan, D. K. Pradhan, K. Arun, N. Santander, T. Reji and R. S. K atiyar, *J. Power Sources.*, 183 (2008) 961-765.
7. Z. L. Liu, A. S. Yu and J. Y. Lee, *Power Sources.*, 81-82 (1999) 416-419.
8. W. M. Liu, G. R. Hu, Z. D. Peng, K. Du, Y. B. Cao and Q. Liu, *Chinese Chem. Lett.*, 22 (2011) 1099-1102.
9. L. L. Liang, K. Du, Z. D. Peng, Y. B. Cao, J. G. Duan, J. J. Jiang and G. R. Hu, *Electrochimica Acta.*, 131 (2014) 82-89.
10. H. Lu, H. Zhou, A. M. Svensson, A. Fossdal, E. Sheridan, S. Lu, F. Vullum-bruer, *Solid State Ion.*, 249-250 (2013) 105-111.
11. G. R. Hu, Y. J. Liu, Z. D. Peng, K. Du, X. G. Gao, *The Chinese J. Nonferrous Met.*, 17 (2007) 1, 59-67.
12. L. J. Li, X. H. Li, Z. X. Wang, H. J. Guo, P. Yue, W. Chen and L. Wu, *Powder. Technol.*, 206 (2011) 353-357.
13. S. Gopukumar, K. Y. Chung, K. B. Kim, *Electrochimica Acta.*, 49 (2004) 803-810.
14. J. Cho, G. Kim and H. S. Lim, *J. Electrochem. Soc.*, 146 (1999) 10, 3571-3576.
15. S. H. Park, K. S. Park, Y. K. Sun, K. S. Nahm, Y. S. Leec, M. Yoshio, *Electrochimica Acta.*, 46 (2001) 1215-1222.
16. Y. K. Sun, J. L. Dong, J. L. Yun, H. C. Zong and S. T. Myung, *Appl. Mater. Interfaces.*, 5 (20 13) 11434-11440.
17. S. W. Woo, S. T. Myung, H. Bang, D. W. Kim and Y. K. Sun, *Electrochimica Acta.*, 54 (2009) 3851-3856.
18. J. Yang and Y. Y. Xia, *Appl. Mater. Interfaces.*, 8 (2016) 1297-1308.
19. F. Wu, J. Tian, Y. F. Su, J. Wang, C. Z. Zhang, L. Y. Bao, T. He, J. H. Li and S. Chen, *Appl. Mater. Interfaces.*, 7 (2015) 7702-7708.
20. P. Yue, Z. X. Wang, H. J. Guo, X. H. Xiong and X. H. Li, *Electrochimica Acta.*, 92 (2013)1-8.
21. L. J. Li, Z. Y. Chen, Q. B. Zhang, M. Xu, X. Zhou, H. L. Zhu and K. L. Zhang, *J. Mater. Chem. A.*, 3 (2015) 894-904.